HHS Public Access

Author manuscript

Nat Methods. Author manuscript; available in PMC 2016 March 01.

Published in final edited form as:

Nat Methods. 2011 May ; 8(5): 393–399. doi:10.1038/nmeth.1596.

Two-photon absorption properties of fluorescent proteins

Mikhail Drobizhev[1], **Nikolay S. Makarov**[1,4], **Shane E. Tillo**[2,5], **Thomas E. Hughes**[2], and **Aleksander Rebane**[1,3]

[1]Department of Physics, Montana State University, Bozeman, Montana, USA.

[2]Department of Cell Biology and Neuroscience, Montana State University, Bozeman, Montana, USA.

[3]National Institute of Chemical Physics and Biophysics, Akadeemia tee, Tallinn, Estonia.

Abstract

Two-photon excitation of fluorescent proteins is an attractive approach for imaging living systems. Today researchers are eager to know which proteins are the brightest, and what the best excitation wavelengths are. Here we review the two-photon absorption properties of a wide variety of fluorescent proteins, including new far-red variants, to produce a comprehensive guide to choosing the right FP and excitation wavelength for two-photon applications.

Two-photon laser scanning microscopy (2PLSM)[1,2] of cells and tissues expressing fluorescent proteins is becoming a powerful tool for biological studies at different levels of organization[2-4]. The advantages of two-photon excitation (2PE) include reduced out-of-focus photobleaching, less autofluorescence, deeper tissue penetration, and intrinsically high three-dimensional resolution[1,2]. 2PLSM should make it possible to obtain even better optical recordings of ion concentration and cell signaling with genetically targeted sensors [5,6]. Two-photon excitation of fluorescent proteins can also be considered as potentially advantageous in the contexts of genetically targeted deep photodynamic therapy or chromophore-assisted light inactivation[6], three-dimensional optical memory[7], as well as superresolution (sub-diffraction limited) imaging techniques, such as stimulated emission depletion[8], photo-activated localization microscopy, and stochastic optical reconstruction microscopy[9].

To fully realize the potential of 2PE of the fluorescent proteins, it is important to know their two-photon absorption (2PA) spectra, cross sections, σ_2, and 2PE action cross sections, or brightness, σ_2', ($\sigma_2' = \sigma_2 \times \phi$, where ϕ is the fluorescence quantum yield). The linear, one-photon absorption (1PA) spectra and extinction coefficients of many fluorescent proteins have been described and reviewed[5,6,10] (**Supplementary Table 1** online), but the 1PA properties are not sufficient to predict the key 2PA properties such as optimum excitation wavelength and maximum brightness (**Box 2**).

Correspondence should be addressed to M.D. (drobizhev@physics.montana.edu)..

[4]Present address: School of Chemistry and Biochemistry, Georgia Institute of Technology, Atlanta, Georgia.

[5]Present address: Vollum Institute, Oregon Health and Science University, Portland, Oregon.

Here we present a systematic characterization of the 2PA properties of 48 different fluorescent proteins using the same experimental setup, common 2PA reference standards, and an all-optical method for measuring mature chromophore concentration[11] (**Supplementary Methods** online). Briefly, we use a relative fluorescence method with femtosecond excitation and coumarin 485 (Exciton), coumarin 540A (Exciton), rhodamine 610 (Exciton), fluorescein (Aldrich), and styryl 9M (Aldrich) as 2PA standards[12], which eliminates the necessity to calibrate the laser parameters. The power dependence of the fluorescence signal was quadratic for all data presented, assuring that the spectra represent pure 2PA. Further, the spectra were collected in a much broader range (550 – 1,400 nm) than commonly reported, which reveals new optimal wavelengths for excitation and provides new insights into the relation of 2PA properties with protein structure.

To sample broadly, and include the proteins commonly used with one-photon excitation, we combine previously reported spectra of some blue (EBFP series), cyan (ECFP and mCerulean), teal (mTFP series), green (EGFP, mWasabi, mAmetrine), orange and red (DsRed, mRFP, and Fruits series) fluorescent proteins[11,13] with newly obtained results for a number of other fluorescent proteins, including the most promising far-red variants, such as mRaspberry, E2-Crimson, mKate, mKate2, tdKatushka2, mGrape3, mNeptune, eqFP650, and eqFP670. The 2PA spectrum (presented in absolute cross section values per mature chromophore) represents the fundamental molecular property of a fluorescent protein, property that could strongly constrain its utility in any two-photon application. The data presented here is an important first step in determining which proteins are brightest upon two-photon excitation and at what wavelengths, but there are other factors, such as expression rate, photostability, photoswitching efficiency, or ability to generate singlet oxygen, that need to be considered while selecting the right mutant for a particular two-photon application.

Two-photon versus one-photon absorption properties

There are several different classes of fluorescent proteins that are usually grouped according to their chromophore structure. These classes vary tremendously in terms of their absorption and fluorescence properties. Similarly, large variations are observed in 2PA spectra (**Fig. 1** and **Supplementary Figs. 1 - 12** online). Because the chromophore in fluorescent proteins is not centrosymmetric, the parity selection rules for one- and two-photon transitions are relaxed[14]. As a result, the same bands should appear in both one- and two-photon absorption spectra, although with different relative intensities. An overlap between 1PA and 2PA spectra is generally apparent for the longest-wavelength absorption band, corresponding to the first electronic, $S_0 \rightarrow S_1$, transition (**Box 2** and **Fig. 2**). For the neutral chromophores found in EBFP2.0, mAmetrine, ECFP, and mBlueberry1, the corresponding 1PA and 2PA peaks coincide rather well. In the anionic chromophores of EGFP, Citrine, mOrange, DsRed2, and TagRFP, however, there is a distinct blue shift of the 2PA band relative to the 1PA band. This observation, previously ascribed to an enhancement of certain vibronic transitions in 2PA spectrum[11,15], illustrates why the optimal 2PA excitation wavelength cannot in general be deduced from the 1PA peak wavelength.

The most striking difference between the 2PA and 1PA spectra is however the appearance of a strong two-photon absorption in the region of wavelengths much shorter than those of the $S_0 \rightarrow S_1$ transition, where the 1PA is extremely weak. These recently observed 2PA features of fluorescent proteins[14] belong to higher electronic $S_0 \rightarrow S_n$ transitions, which have been predicted theoretically for various types of chromophores[16] (**Supplementary Fig. 13** online). The $S_0 \rightarrow S_n$ shorter-wavelength 2PA transitions can be very intense due to the resonance enhancement effect[14] (**Box 2**). Indeed, in some chromophores, including those of Citrine, mOrange, mBlueberry1, DsRed2, and TagRFP, this enhancement is so strong that optimal excitation is found at wavelengths much shorter than what one would expect based on the 1PA properties alone (**Fig. 1**). In the spectra of red and far-red proteins these $S_0 \rightarrow S_n$ transitions occur at 700 - 770 nm, matching well with the tuning range of femtosecond Ti:sapphire lasers and thus offering new opportunities with already existing commercial 2PLSM systems[13,17]. For example, excitation of the higher $S_0 \rightarrow S_n$ transition of TagRFP simultaneously with the first, $S_0 \rightarrow S_1$, transition of mKalama1 makes dual-color two-photon imaging possible with a single excitation laser wavelength[13]. Alternatively, two proteins with very different Stokes shifts can be used for this purpose[18].

Compared to a regular dye in solution, the chromophore of a fluorescent protein is buried within a complex, spatially organized protein environment that influences the optical properties of the chromophore through electrostatic interactions[19]. Recently, it has been shown that different hues in a series of mutants that contain the same (DsRed-type) chromophore are caused by variations in the local electric field inside the beta barrel[20]. Interestingly, the shifts of the 1PA peak wavelength are accompanied by only small changes in the extinction coefficient (**Fig. 3a**). The local electrostatic environment also influences the 2PA properties, but with the important difference that the shift of the peak absorbance is accompanied by large changes in 2PA cross section (**Fig. 3b**). This is because the 2PA cross section is much more sensitive to the local electric field variations (**Box 3**, **Fig. 4**). For example, Citrine is as bright as EGFP upon one-photon excitation, but it is much dimmer than EGFP upon two-photon excitation. This effect could be due to the change of the local field at the chromophore site caused by the high polarizability of a nearby stacking tyrosine 203 residue[21].

Choosing the protein and laser for two-photon excitation

Table 1 summarizes the most relevant 2PA properties of a representative set of fluorescent proteins (see **Supplementary Table 2** online for all the proteins studied). Comparison of the data reveals a remarkable variability: the maximum 2PA cross section (σ_2) and brightness (σ_2') change over two orders of magnitude (**Fig. 1** and **Table 1**). These are much larger differences than those observed for one-photon extinction (ε) which changes at most by eight fold (from 10,800 (mBlueberry1) to 85,600 M^{-1} cm^{-1} (DsRed2)). This means that identifying the right fluorescent protein for a particular 2PA application is crucial for success.

If we concentrate only on two-photon brightness, several proteins stand out as good potential two-photon probes in the Ti:sapphire tuning range. Among the proteins fluorescing in the blue-green region, the members of mTFP series are twice as bright as EGFP when

excited at 870 - 920 nm. In the yellow-orange region of fluorescence, mOrange can be efficiently excited near 730 nm, while TagRFP, tdTomato, DsRed, mKate, mKate2, mKate S158A, mKate S158C, tdKatushka2, and mNeptune show quite bright red fluorescence when excited at 730 – 770 nm.

Several proteins offer useful 2PA properties beyond the common range of Ti:sapphire lasers. In particular, those with orange to far-red fluorescence can be excited efficiently at wavelengths between 1,000 and 1,200 nm, where there is relatively little tissue or water absorption, weak tissue scattering, and vanishing small amounts of tissue autofluorescence[1] (**Fig. 5**). There is a good match between the 2PA peak of tdTomato and tdKatushka2 and minimum attenuation of the tissue in the spectral range from 1,000 to 1,150 nm. While tdKatushka2 is not as bright as tdTomato, its fluorescence spectrum is red shifted with respect to that of tdTomato (**Fig. 5**), fitting better to the highest transparency range. Although the region of 1,000 – 1,150 nm is inaccessible to standard Ti:sapphire lasers, there are other laser solutions currently available, such as femto- and picosecond Nd- and Yb-doped fiber and glass lasers.

Why do the published 2PE cross sections vary so much?

An accurate measurement of the absolute 2PA cross section remains a technically demanding task requiring careful independent experimental evaluation of a number of parameters, each of which has a particular experimental error that contributes to uncertainty in the cross section value. The pioneering works by the Webb[1,2,22,23], Schmidt[15], and Kleinfeld[3] groups reported the 2PE action cross section spectra of ECFP, EGFP, EYFP, and DsRed, measured within the typical spectral range of a Ti:sapphire laser. More 2PE[4,11,13,14,18,24-26] and 2PA[27] spectra followed, but the absolute 2PE cross sections obtained even for the same protein varied dramatically. For example, the peak σ_2' value of EGFP has been reported to be 1.5[27], 20[24], 40[15], 60[22], 180[18], 180[2], and 300 (for mEGFP)[26] GM. Such discrepancies may be attributed to several potential sources of experimental errors. First, measurements based on two-photon excited fluorescence are usually more accurate than nonlinear transmission techniques (NLT, including Z-scan, pump-probe, etc.) because they rely on zero-background detection and require much less excitation power and lower concentration of chromophores. The high levels of excitation used in NLT can initiate other spurious nonlinear optical processes such as thermal lensing, stimulated emission and scattering, resulting in underestimated 2PA cross sections[28].

Most of the reported cross sections values were obtained by using 2PE fluorescence in combination with 2PA standards. In several works these measurements were performed relative to fluorescein or rhodamine B, but the actual values for these reference dyes vary in the literature[12,29]. This can explain the difference between the EGFP peak cross section, σ_2' = 29 GM, obtained here using the fluorescein value of $\sigma_2 = 16 \pm 2$ GM at 920 nm[12], and σ_2' = 41 GM reported by Blab et al.[15] that was based upon a higher value ($\sigma_2 = 26 \pm 8$ GM) for fluorescein at the same wavelength[29].

Finally, most measurements have been complicated by an uncertainty over the actual concentration of the mature chromophore in a protein sample. Typically the concentration is

measured by Bicinchoninic Acid protein assay (BCA) or alkaline denaturation methods. Both can introduce errors, especially if the protein folds/matures poorly or/and the chromophore is unstable under alkaline denaturating conditions[30]. This can be circumvented by using an all-optical approach[11] that relates the fluorescence lifetime and quantum yield to the extinction coefficient (**Supplementary Methods** and **Supplementary Fig. 14** online). Comparison of our measurements of mBanana[11] and those reported previously[31] reveals that this protein has an order of magnitude higher extinction coefficient than previously thought because it appears that only a small portion of the protein matures to form the chromophore.

While the last 15 years of work have produced a remarkably wide range of reported cross sections values for EGFP and other commonly used proteins, there is an emerging consensus for some of the proteins. The cross section of EGFP at 850 nm recently obtained by Herz *et al.*[4] is in perfect agreement with our result at the same wavelength, and recent data by Hashimoto *et al.*[24] on EGFP, BFP, and ECFP are also consistent with our measurements (**Supplementary Table 2** online).

Remaining challenges

A great deal of effort has been devoted to optimizing one-photon properties of fluorescent proteins, but surprisingly little attention has been paid to creating brighter mutants for two-photon applications. The recently developed model of the effect of local protein environment on 2PA (**Box 3**) should make it possible to increase the 2PA cross section by manipulating the strength and direction of the electric field inside the barrel. New generations of mutants with even brighter two-photon fluorescence will inevitably be created. Large 2PA cross sections and quantum yields are only part of the solution however. In 2PLSM, the photostability of the probe is a serious constraint. To date, there is very limited information on the nonlinear multiphoton photobleaching of fluorescent proteins, and it is often difficult to compare measurements directly because the bleaching rate depends upon several laser parameters in a complex way[4,32-37] and can vary dramatically between fluorescent proteins[38].

At the rather high excitation intensities usually required for 2PLSM (10^5 – 10^7 W/cm^2 at the sample), the photobleaching rate rises with laser intensity more steeply than the expected quadratic function [4,32,33]. This means that lowering the peak power, while raising the repetition rate, can reduce total photodamage while producing the same fluorescence signal[34]. One possible explanation for the very steep power dependence of the photobleaching could be a further (stepwise) absorption from a long-lived triplet state[35]. This is consistent with the observation that lowering the repetition rate, while maintaining the same peak power, can be beneficial[35], although the improvement comes with the cost of longer acquisition times.

The photophysical mechanisms of nonlinear photobleaching remain unclear. The first step will be to carefully characterize the multiphoton photobleaching rates of a broad set of fluorescent proteins, which should then lead to a structure – property model that can be used to develop new variants more suitable for 2PLSM and other challenging applications. There is empirical evidence that reducing the photon energy (i.e. increasing wavelength) often

provides better photostability in 2PLSM. The photobleaching of DsRed slows down by an order of magnitude when the excitation wavelength is shifted to the red, from 750 to 950 nm[32]. Similarly, excitation of EGFP at 920 nm provides the two-fold improvement compared to 850 nm[4], and the red protein (tdRFP) is much more stable upon 1,100-nm excitation than the green protein (EGFP) excited at 850 or 920 nm[4]. These observations, and the high 2PE brightness near 1,050 – 1,150 nm of mOrange, TagRFP, tdTomato, DsRed, tdKatushka2, and mKate2 indicate that these bright 2PE probes can offer new opportunities for deep tissue imaging.

Supplementary Material

Refer to Web version on PubMed Central for supplementary material.

Acknowledgments

This work was supported by the National Institute of General Medical Sciences, grant R01 GM086198. We thank Mr. B. H. Davis for technical help and Drs. R. Campbell (University of Alberta, Edmonton, Canada), D. M. Chudakov (Shemyakin and Ovchinnikov Institute of Bioorganic Chemistry, Moscow Russia), M. Lin (Stanford University, Stanford, California, USA), and R. Y. Tsien (University of California, San Diego, La Jolla, California, USA) for kindly providing us cDNA of different fluorescent proteins.

References

1. Xu C, Zipfel W, Shear JB, Williams RM, Webb WW. Multiphoton fluorescence excitation: New spectral windows for biological nonlinear microscopy. Proc. Natl. Acad. Sci. USA. 1996; 93:10763–10768. [PubMed: 8855254] [An important presentation of the 2PLSM method with an emphasis on 2PA spectroscopy of biologically relevant fluorescent dyes. Here, the two-photon absorption spectra of two GFPs (wt-GFP and S65T mutant) were presented for the first time.]
2. Zipfel WR, Williams RM, Webb WW. Nonlinear magic: multiphoton microscopy in the biosciences. Nat. Biotech. 2003; 21:1369–1377.
3. Tsai PS, et al. All-optical histology using ultrashort laser pulses. Neuron. 2003; 39:27–41. [PubMed: 12848930]
4. Herz J, et al. Expanding two-photon intravital microscopy to the infrared by means of optical parametric oscillator. Biophys. J. 2010; 98:715–723. [PubMed: 20159168]
5. Tsien RY. The green fluorescent protein. Ann. Rev. Biochem. 1998; 67:509–544. and references therein. [PubMed: 9759496] [This early review of the fluorescent proteins describes 1PA properties of GFPs with different chromophores and identifies the need of more studies of their 2PA properties.]
6. Chudakov DM, Matz MV, Lukyanov S, Lukyanov KA. Fluorescent proteins and their applications in imaging living cells and tissues. Physiol. Rev. 2010; 90:1103–1163. and references therein. [PubMed: 20664080]
7. Adam V, et al. Data storage based on photochromic and photoconvertible fluorescent proteins. J. Biotech. 2010; 149:289–298.
8. Moneron G, Hell SW. Two-photon excitation STED microscopy. Opt. Express. 2009; 17:14567–14573. [PubMed: 19687936]
9. Vaziri A, Tang J, Shroff H, Shank CV. Multilayer three-dimensional super resolution imaging of thick biological samples. Proc. Natl. Acad. Sci. USA. 2008; 105:20221–20226. [PubMed: 19088193]
10. Shaner NC, Steinbach PA, Tsien RY. A guide to choosing fluorescent proteins. Nat. Methods. 2005; 2:905–909. [PubMed: 16299475]
11. Drobizhev M, Tillo S, Makarov NS, Hughes TE, Rebane A. Absolute two-photon absorption spectra and two-photon brightness of orange and red fluorescent proteins. J. Phys. Chem. B. 2009; 113:855–859. [PubMed: 19127988]

12. Makarov NS, Drobizhev M, Rebane A. Two-photon absorption standards in the 550--1600 nm excitation wavelength range. Opt. Express. 2008; 16:4029–4047. [PubMed: 18542501] [This paper presents a large number of 2PA standards that can be used to measure the spectra of new fluorophores with high accuracy in a very wide spectral range.]
13. Tillo SE, Hughes TE, Makarov NS, Rebane A, Drobizhev M. A new approach to dual-color two-photon microscopy with fluorescent proteins. BMC Biotech. 2010; 10 Art. # 6.
14. Drobizhev M, Makarov NS, Hughes T, Rebane A. Resonance enhancement of two-photon absorption in fluorescent proteins. J. Phys. Chem. B. 2007; 111:14051–14054. [PubMed: 18027924]
15. Blab GA, Lommerse PHM, Cognet L, Harms GS, Schmidt T. Two-photon excitation action cross-sections of the autofluorescent proteins. Chem. Phys. Lett. 2001; 350:71–77.
16. Nifosi R, Luo Y. Predictions of novel two-photon absorption bands in fluorescent proteins. J. Phys. Chem. B. 2007; 111:14043–14050. [PubMed: 18027922]
17. Nguyen QT, et al. An *in vivo* biosensor for neurotransmitter release and *in situ* receptor activity. Nat. Neurosci. 2010; 13:127–132. [PubMed: 20010818]
18. Kawano H, Kogure T, Abe Y, Mizuno H, Miyawaki A. Two-photon dual-color imaging using fluorescent proteins. Nat. Methods. 2008; 5:373–374. [PubMed: 18446153]
19. Shu X, Shaner NC, Yarbrough CA, Tsien RY, Remington SJ. Novel chromophores and buried charges control color in mFruits. Biochem. 2006; 45:9639–9647. [PubMed: 16893165] [This paper suggests the effect of local electrostatic fields on the different absorption and fluorescence properties of red fluorescent proteins, an effect that was later quantitatively demonstrated with 2PA spectroscopy in Ref. 20.]
20. Drobizhev M, Tillo S, Makarov NS, Hughes TE, Rebane A. Color hues in red fluorescent proteins are due to internal quadratic Stark effect. J. Phys. Chem. B. 2009; 113:12860–12864. [PubMed: 19775174]
21. Wachter RM, Elsliger M-A, Kallio K, Hanson GT, Remington SJ. Structural basis of spectral shifts in the yellow-emission variants of green fluorescent protein. Struct. 1998; 6:1267–1277.
22. Heikal AA, Hess ST, Webb WW. Multiphoton molecular spectroscopy and excited-state dynamics of enhanced green fluorescent protein (EGFP): Acid-base specificity. Chem. Phys. 2001; 274:37–45.
23. Heikal AA, Hess ST, Baird GS, Tsien RY, Webb WW. Molecular spectroscopy and dynamics of intrinsically fluorescent proteins: Coral red (dsRed) and yellow (Citrine). Proc. Nat. Acad. Sci. USA. 2000; 97:11996–12001. [PubMed: 11050231]
24. Hashimoto H, et al. Measurement of two-photon excitation spectra of fluorescent proteins with nonlinear Fourier-transform spectroscopy. Appl. Opt. 2010; 49:3323–3329. [PubMed: 20539351]
25. Piatkevich KD, et al. Monomeric red fluorescent proteins with a large Stokes shift. Proc. Natl. Acad. Sci. USA. 2010; 107:5369–5374. [PubMed: 20212155]
26. Rizzo MA, Springer G, Segawa K, Zipfel WR, Piston DW. Optimization of pairings and detection conditions for measurements of FRET between cyan and yellow fluorescent proteins. Microsc. Microanal. 2006; 12:238–254. [PubMed: 17481360]
27. Hosoi H, Yamaguchi S, Mizuno H, Miyawaki A, Tahara T. Hidden electronic excited state of enhanced green fluorescent protein. J. Phys. Chem. B. 2008; 112:2761–2763. [PubMed: 18275187]
28. Oulianov DA, Tomov IV, Dvornikov AS, Rentzepis PM. Observations on the measurement of two-photon absorption cross-section. Opt. Comm. 2001; 191:235–243.
29. Albota MA, Xu C, Webb WW. Two-photon fluorescence excitation cross sections of biomolecular probes from 690 to 960 nm. Appl. Opt. 1998; 37:7352–7356. [PubMed: 18301569]
30. Kredel S, et al. Optimized and far-red-emitting variants of fluorescent protein eqFP611. Chem. Biol. 2008; 15:224–233. [PubMed: 18355722]
31. Shaner NC, et al. Improved monomeric red, orange and yellow fluorescent proteins derived from Discosoma sp. red fluorescent protein. Nat. Biotech. 2004; 22:1567–1572.
32. Marchant JS, Stutzmann GE, Leissring MA, LaFerla FM, Parker I. Multiphoton-evoked color change of DsRed as an optical highlighter for cellular and subcellular labeling. Nat. Biotech. 2001; 19:645–649.

33. Chen T-S, Zeng S-Q, Luo Q-M, Zhang Z-H, Zhou W. High-order photobleaching of Green Fluorescent Protein inside live cells in two-photon excitation microscopy. Biochem. Biophys. Res. Comm. 2002; 291:1272–1275. [PubMed: 11883955]
34. Ji N, Magee JC, Betzig E. High-speed, low-photodamage nonlinear imaging using passive pulse splitters. Nat. Methods. 2008; 5:197–202. [PubMed: 18204458] [Currently, one of the greatest constraints in two-photon imaging with fluorescent proteins is rapid photobleaching. This paper describes a novel optical solution to at least part of the problem.]
35. Donnert G, Eggeling C, Hell SW. Major signal increase in fluorescence microscopy through dark-state relaxation. Nat. Methods. 2007; 4:81–86. [PubMed: 17179937]
36. Kawano H, et al. Attenuation of photobleaching in two-photon excitation fluorescence from green fluorescent protein with shaped excitation pulses. Biochem. Biophys. Res. Comm. 2003; 311:592–596. [PubMed: 14623311]
37. Field JJ, et al. Optimizing the fluorescent yield in two-photon laser scanning microscopy with dispersion compensation. Opt. Express. 2010; 18:13661–13672. [PubMed: 20588500]
38. Patterson GH, Knobel SM, Sharif WD, Kain SR, Piston DW. Use of the Green Fluorescent Protein and its mutants in quantitative fluorescence microscopy. Biophys. J. 1997; 73:2782–2790. [PubMed: 9370472]
39. Ritz J-P, et al. Optical properties of native and coagulated porcine liver tissue between 400 and 2400 nm. Lasers Surg. Med. 2001; 29:205–212. [PubMed: 11573221]
40. Ai HW, Shaner NC, Cheng Z, Tsien RY, Campbell RE. Exploration of new chromophore structures leads to the identification of improved blue fluorescent proteins. Biochem. 2007; 46:5904–5910. [PubMed: 17444659]
41. Rizzo MA, Springer GH, Granada B, Piston DW. An improved cyan fluorescent protein variant useful for FRET. Nat. Biotech. 2004; 22:445–449.
42. Ai HW, Henderson JN, Remington SJ, Campbell RE. Directed evolution of a monomeric, bright and photostable version of Clavularia cyan fluorescent protein: structural characterization and applications in fluorescence imaging. Biochem. J. 2006; 400:531–540. [PubMed: 16859491]
43. Ai HW, Hazelwood KL, Davidson MW, Campbell RE. Fluorescent protein FRET pairs for ratiometric imaging of dual biosensors. Nat. Methods. 2008; 5:401–403. [PubMed: 18425137]
44. Griesbeck O, Baird GS, Campbell RE, Zacharias DA, Tsien RY. Reducing the environmental sensitivity of yellow fluorescent protein. J. Biol. Chem. 2001; 31:29188–29194. [PubMed: 11387331]
45. Tsutsui H, Karasawa S, Okamura Y, Miyawaki A. Improving membrane voltage measurements using FRET with new fluorescent proteins. Nat. Methods. 2008; 5:683–685. [PubMed: 18622396]
46. Merzlyak EM, et al. Bright monomeric red fluorescent protein with an extended fluorescence lifetime. Nat. Methods. 2007; 4:555–557. [PubMed: 17572680]
47. Yanushevich YG, et al. A strategy for the generation of non-aggregating mutants of Anthozoa fluorescent proteins. FEBS Lett. 2002; 511:11–14. [PubMed: 11821040]
48. Wang L, Jackson WC, Steinbach PA, Tsien RY. Evolution of new nonantibody proteins via iterative somatic hypermutation. Proc. Nat. Acad. Sci. USA. 2004; 101:16745–16749. [PubMed: 15556995]
49. Shcherbo D, et al. Far-red fluorescent tags for protein imaging in living tissues. Biochem. J. 2009; 418:567–574. [PubMed: 19143658]
50. Lin MZ, et al. Autofluorescent proteins with excitation in the optical window for intravital imaging in mammals. Chem. Biol. 2009; 16:1169–1179. [PubMed: 19942140]

Box 1. Glossary of terms

Electronic transitions: The absorption and fluorescence emission of photons by fluorescent protein is due to the system of π-conjugated electrons of the chromophore. Upon excitation, this system moves into an excited, higher energy state. This movement from the initial, or ground, state (S_0) to an excited state (S_1 or S_n) is called an electronic transition, whose frequency is equal to the energy difference between the two states divided by the Planck constant. Higher-energy transitions ($S_0 \rightarrow S_n$) correspond to absorption at shorter (more energetic) wavelengths compared to lowest-energy transition ($S_0 \rightarrow S_1$) which corresponds to the longest wavelength.

Vavilov-Kasha's rule states that fluorescence properties are independent of the mode (one- or two-photon) or wavelength of excitation and thus exciting any state S_n (n = 1, 2, 3,...) will yield the same fluorescence spectrum. When exciting a higher-energy sate S_n (n = 2, 3,..) fluorescence does not occur from that state. Instead, some of the energy is lost in the form of heat (see dashed arrows in the **Fig. 2**) and emission occurs from the lowest excited state S_1.

Stokes shift is the frequency difference between the excitation maximum of the $S_0 \rightarrow S_1$ transition and fluorescence emission maximum of the $S_1 \rightarrow S_0$ transition.

Vibronic transitions: In addition to a change of electronic states upon optical excitation, a vibrational state of a molecule can also change. While in the vibrational ground state atoms mostly occupy their near-equilibrium positions. In a vibrational excited state these atoms start to oscillate (acquire vibration energy) along certain normal coordinates. If both electronic and vibrational states change upon excitation, then this transition corresponds to the molecule acquiring a quantum (or several quanta) of vibrational energy in the electronically excited state that sum to form vibronic transition. This transition always occurs higher in energy (at shorter wavelength) than the pure electronic transition in the absorption spectrum.

Box 2. Anatomy of two-photon absorption spectrum

Two-photon absorption cross section, σ_2, (measured in Goeppert-Mayer units, 1 GM = 10^{-50} cm^4 s) characterizes the probability of the simultaneous absorption of two photons whose energies add up to match the molecular transition energy. Two-photon absorption is governed by different quantum-mechanical rules than one-photon absorption, and, as a result, the 2PA spectra are often much different in shape than their one-photon counterparts, as exemplified in the **Fig. 2** for TagRFP. The 1PA (extinction) spectrum in the region of the $S_0 \rightarrow S_1$ transition (right hand side of the Fig. 2 and right Jablonski diagram) is described by

$$\varepsilon(\nu) = A|\boldsymbol{\mu}_{n1}|^2 g_1(\nu) \qquad (1)$$

where A is a constant, ν is the frequency, $\boldsymbol{\mu}_{10}$ is the matrix element of the electronic transition dipole moment between states S_0 and S_1, $g_1(\nu)$ is the 1PA lineshape function, which includes the distribution of intensity due to vibronic transitions. The 2PA spectrum in the same region is represented, within the two-level approximation, by[14]:

$$\sigma_2(\nu) = B|\Delta\boldsymbol{\mu}_{10}|^2|\boldsymbol{\mu}_{10}|^2 g_2(\nu) \qquad (2)$$

where B is another constant, $\Delta\boldsymbol{\mu}_{10}$ is the difference between permanent dipole moments of the excited (S_1) and ground (S_0) states, $g_2(\nu)$ is the 2PA lineshape function. The shape of the 2PA spectrum, $g_2(\nu)$, is different from the shape of the 1PA spectrum, $g_1(\nu)$, because some vibronic transitions become enhanced in the two-photon process, whereas the pure electronic transition is the strongest in one-photon process. In the $S_0 \rightarrow S_n$ transition region (left hand side of the **Fig. 2**), the 2PA is surprisingly strong. The 1PA in this region is described by

$$\varepsilon(\nu) = A|\boldsymbol{\mu}_{n0}|^2 g_1'(\nu) \qquad (3)$$

where $g_1'(\nu)$ is the 1PA lineshape function for this higher transition, $\boldsymbol{\mu}_{n0}$ is the transition dipole moment connecting states S_0 and S_n. The 1PA is very weak (see **Fig. 2**) because of small absolute value of $\boldsymbol{\mu}_{n0}$. The 2PA, in the three-level approximation[14], reads:

$$\sigma_2(\nu) = B\nu_L^2|\boldsymbol{\mu}_{n1}|^2|\boldsymbol{\mu}_{10}|^2 g_2'(\nu)/(\nu_{10}-\nu_L)^2 \qquad (4)$$

where $\boldsymbol{\mu}_{1n}$ is the transition dipole moment between states S_1 and S_n, $g_2'(\nu)$ is the 2PA lineshape function, ν_{10} is the (peak) frequency of the $S_0 \rightarrow S_1$ transition, ν_L is the laser frequency ($\nu_L = \nu/2$). The 2PA becomes very strong in this region due to large absolute values of $\boldsymbol{\mu}_{10}$, $\boldsymbol{\mu}_{1n}$, and quantum-mechanical effect known as resonant enhancement[14]. Resonant enhancement occurs when the laser frequency, ν_L, approaches from below the energy of the lowest S_1 state, ν_{10}, resulting in fast reduction of denominator in (4).

Box 3. Effect of local internal electric field on optical properties of fluorescent proteins

Because two-photon absorption is governed by different quantum mechanical rules, it reveals different aspects of the chromophore structure and chromophore – protein interactions. Unlike linear extinction ε, which depends only on the transition dipole moment squared, $|\boldsymbol{\mu}_{10}|^2$, 2PA cross section σ_2 is proportional to both $|\boldsymbol{\mu}_{10}|^2$ and $|\Delta\boldsymbol{\mu}_{10}|^2$ (cf. Eq. (2) in **Box 2**). The consequence of this is that σ_2 is sensitive to the electric field present within the protein barrel. Therefore, σ_2 can be manipulated by changing the electrostatic environment of the chromophore. For example, in a series of Fruits, all possessing the same chromophore but different environment, 1PA extinction coefficient vary only very slightly, but 2PA cross section increases very fast when $|\Delta\boldsymbol{\mu}_{10}|$ increases (**Fig. 5**).

The chromophore of a fluorescent protein has a permanent dipole moment in both the ground ($\boldsymbol{\mu}_0$) and excited ($\boldsymbol{\mu}_1$) states. Because of the high mobility of the π-electronic cloud, the $S_0 \rightarrow S_1$ transition has a certain charge-transfer character, resulting in a difference between permanent dipoles ($\Delta\boldsymbol{\mu}_{10} = \boldsymbol{\mu}_1 - \boldsymbol{\mu}_0 \neq 0$). Another important property of the liable π-electron system of the chromophore is that the charge density easily redistributes upon application of external electric field $\boldsymbol{E}$, thus resulting in an additional, induced component of the dipole moment $\boldsymbol{\mu}^{\text{ind}}$. This induced portion of the dipole is related to the electric field through polarizability coefficient (more generally, tensor) α: $\boldsymbol{\mu}^{\text{ind}} = \alpha\,\boldsymbol{E}$. If the polarizabilities in the ground (α_0) and excited (α_1) states are different, the change of induced dipole moment $\Delta\boldsymbol{\mu}^{\text{ind}}_{10}$ will contribute to the total change of dipole moment: $\Delta\boldsymbol{\mu}_1 = \Delta\boldsymbol{\mu}^0_{10} + ½\,\Delta\boldsymbol{\mu}^{\text{ind}}_{10} = \Delta\boldsymbol{\mu}^0_{10} + ½\,(\alpha_1 - \alpha_0)\,\boldsymbol{E}$, where index 0 in $\Delta\boldsymbol{\mu}^0_{10}$ corresponds to “zero field” situation. This dependence makes $\Delta\boldsymbol{\mu}_{10}$ sensitive to the electric field. This mechanistic picture of how the chromophore electronic structure is tuned by its environment makes strong predictions for creating better fluorescent proteins for two-photon applications: One can obtain a strong gain in peak 2PA cross section upon increasing of $|\Delta\boldsymbol{\mu}_{10}|$ (which follows the changes of $\boldsymbol{E}$, or, more accurately, projection of $\boldsymbol{E}$ on $\Delta\boldsymbol{\mu}_{10}$). In fluorescent proteins, $\boldsymbol{E}$ can be altered by changing certain charged amino acids, or the hydrogen bonding network, on the axis of the chromophore dipole.

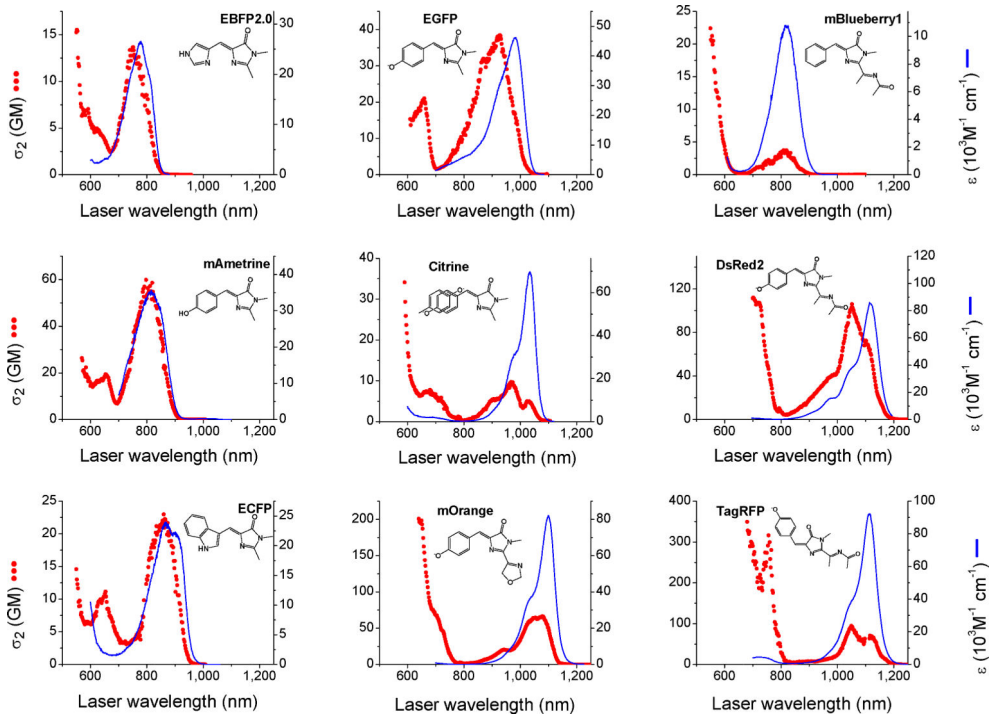

Figure 1.

Comparison of one-photon and two-photon absorption spectra of fluorescent proteins with different chromophores. Two-photon absorption spectra (red symbols, left axis) are presented versus laser wavelength, used for excitation. For comparison purposes, in one-photon absorption spectra (blue lines, right axis) the actual excitation wavelength is multiplied by a factor of two. All spectra are presented in absolute values determined per mature chromophore. Reproduced in part from Ref.[11]. Copyright 2009 American Chemical Society.

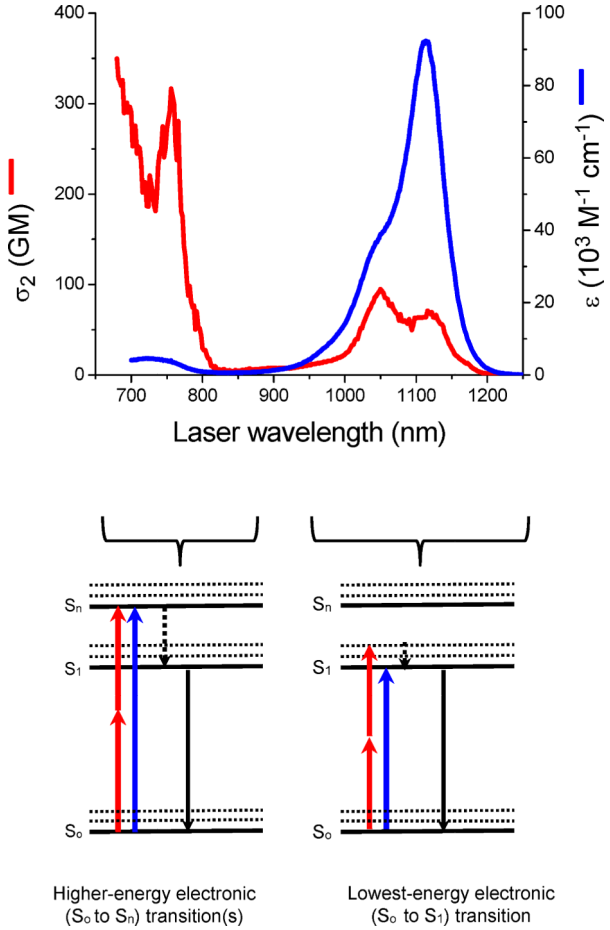

Figure 2.

(Should be placed in **Box 2**). Upper part: One-photon absorption and two-photon absorption spectra of TagRFP. Lower part: Jablonski diagram of 1PA and 2PA transitions.

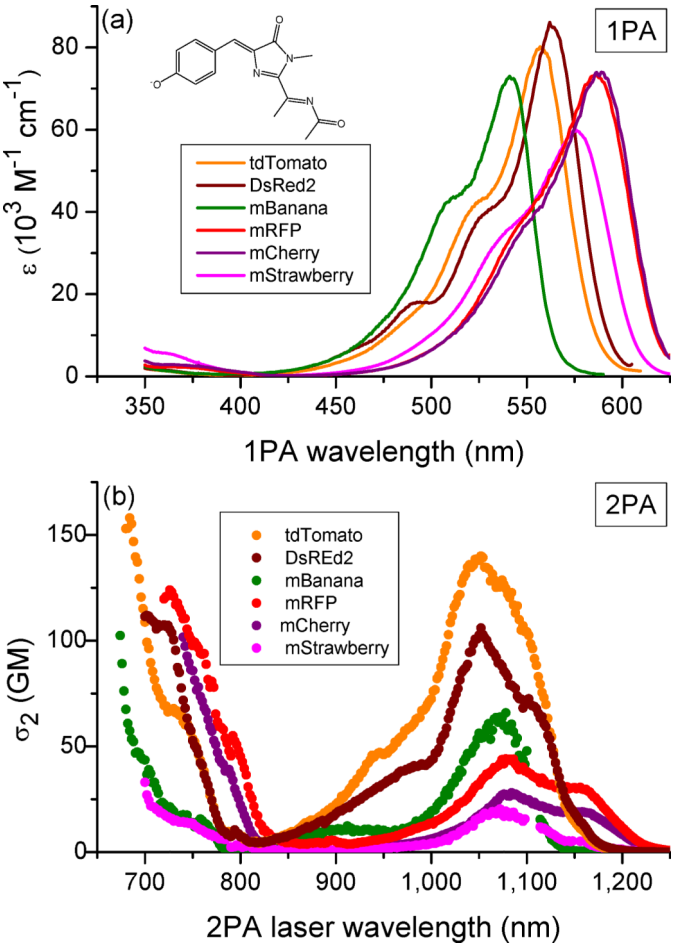

Figure 3.

1PA (**a**) and 2PA (**b**) spectra of the Fruit series of fluorescent proteins. Adopted from Ref.[11]. Copyright 2009 American Chemical Society.

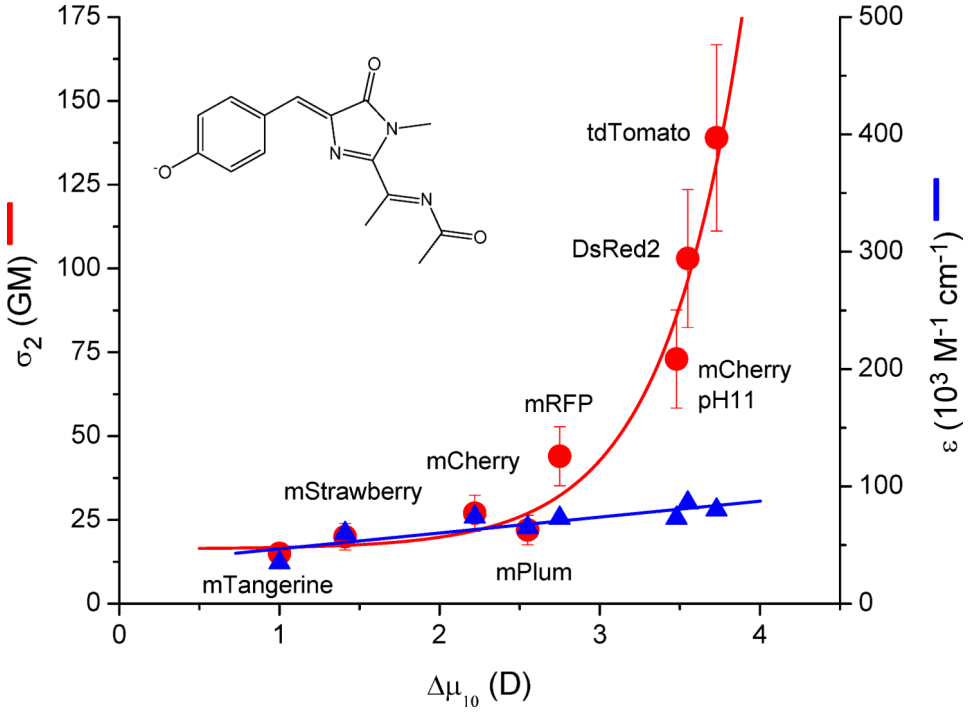

Figure 4.

(Should be placed in **Box 3**). Dependence of 2PA peak cross section and 1PA peak extinction on the change of permanent dipole moment of chromophore upon excitation, $|\Delta\boldsymbol{\mu}_{10}|$ in the of Fruit series.

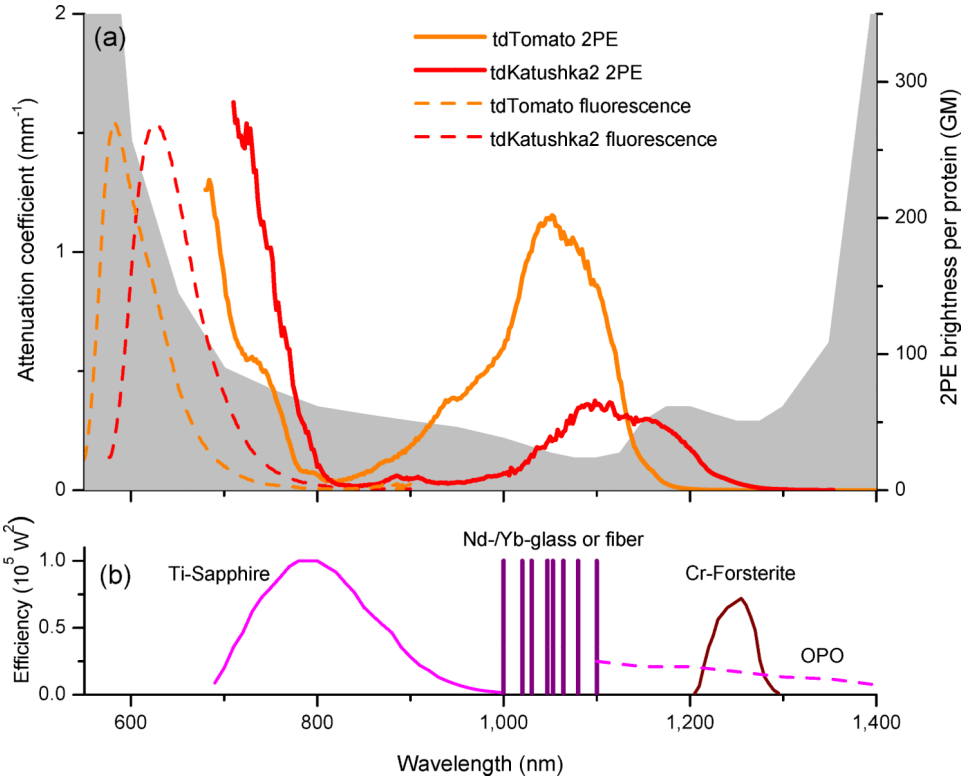

Figure 5.

Matching of two-photon excitation spectra of red fluorescent proteins with the optimum tissue transparency and with the wavelengths of some short-pulse laser systems. (**a**) Typical tissue transparency window (Ref.[39], filled gray) presented as attenuation coefficient, left y-axis; 2PE brightness spectra per protein chain of tdTomato and tdKatushka2, right y-axis; and their corresponding normalized fluorescence spectra. (**b**) Effective laser efficiency relevant to two-photon excitation (average power squared divided by repetition rate and pulse duration) of several commercial femtosecond lasers.

Table 1

Summary of the 2PA properties of representative fluorescent proteins. Two-photon absorption cross section (σ_2), two-photon brightness (σ_2'), both per mature protein are presented in two spectral regions, corresponding to the short- and long-wavelength transitions.

	Short-wavelength band			Long-wavelength band		
Protein	**λ_{2PA} (nm)**	**σ_2 (GM)**	**$\sigma_2 \times \phi$ (GM)**	**λ_{2PA} (nm)**	**σ_2 (GM)**	**$\sigma_2 \times \phi$ (GM)**
EBFP2.0[41]	552	16	11	750	13	9.2
ECFP (Clontech)	550	15	7.8	857	23	12
Cerulean[41]	550	27	16	858	23	13
mTFP1.0[42]	667	6.4	5.4	875	70	59
EGFP (Clontech)	660	22	17	927	39	30
mAmetrine[43]	655	19	13	809	56	40
Citrine[44]	590	34	23	968	10	6.7
mKok[45]	686	93	67	1044	41	30
mOrange[31]	640	200	140	1080	67	47
TagRFP[46]	759	300	130	1050	95	42
tdTomato[31]	684	316	228	1050	278	200
DsRed2[47]	700	112	79	1050	103	73
mCherry[31]	740	101	24	1080	27	6.4
mRaspberry[48]	704	346	65	1118	31	5.8
mPlum[48]	724	114	15	1105	22	2.9
tdKatushka2[49]	710	645	285	1100	143	63
mKate2[49]	712	216	91	1140	72	30
mNeptune[50]	750	335	57	1105	70	12

Note: To obtain $\sigma 2$ and $\sigma 2$' per chromophore in the case of dimers, one has to take one-half of the corresponding values presented in the **Table**.